IFAC Conference on Advances in PID Control
PID'12
Brescia (Italy), March 28-30, 2012

A Cascade PID-PD Controller for a Hybrid Piezo-Hydraulic Actuator in Camless Internal Combustion Engines

Paolo Mercorelli

Institut für Produkt- und Prozessinnovation
Leuphana Universität Lüneburg
Volgershall 1, D-21339 Lüneburg, Germany
Tel.: +49-(0)4131.677-5434, Fax: +49-(0)4131.677-5300

mercorelli@uni.leuphana.de, mercorelli@ing.unisi.it

Abstract: This paper deals with a hybrid actuator composed by a piezo and a hydraulic part and with a cascade PID-PD control structure for camless engine motor applications. The idea is to use the advantages of both, the high precision of the piezo and the force of the hydraulic part. In fact, piezoelectric actuators (PEAs) are commonly used for precision positionings, despite PEAs present nonlinearities, such as hysteresis, saturations, and creep. In the control problem such nonlinearities must be taken into account. In this paper the Preisach dynamic model with the above mentioned nonlinearities is considered together with a cascade PID-PD controller which is realized through sliding surfaces. Simulations with real data are shown.

Keywords: PID controllers, Lyapunov's approach, piezo actuators

1. INTRODUCTION

In the last few years, variable engine valve control in camless systems has attracted a lot of attention because of its ability to reduce pumping losses (work required to draw air into the cylinder under part-load operation) and to increase torque performance over a wider rage than conventional spark-ignition engine. Variable valve timing also allows control of internal exhaust gas recirculation, thus improving fuel economy and reducing NOx emissions. Besides mechanical and hydraulic variable valvetrain options, electromagnetic valve actuators have been reported in the past. Theoretically, electromagnetic valve actuators offer the highest potential to improve fuel economy due to their control flexibility. In real applications, however, the electromagnetic valve actuators developed so far mostly suffer from high power consumption and other control problems. This kind of actuators presents a high value of inductance which can generate some problems of the electromagnetic compatibility with the environment. Therefore, innovative and alternative concepts are required to reduce the losses and drawbacks while keeping a high actuator dynamic which is characterized by high value of velocity and generated force. The idea which this paper presents is to use hybrid actuator composed by a piezo and a hydraulic part in order to take advantages of both, the high precision and velocity of the piezo and the force of the hydraulic part. Moreover, piezo actuators present in general less problems of electromagnetic compatibility due to the quasi absence of the inductance effects. The main advantage of PA is nanometer scale, high stiffness, and fast response. However, since PA has nonlinear property which is called hysteresis effect, it leads to inaccuracy in positioning control with high precise performance. PID regulators are very often applied in industrial application. Recently, variable engine valve control has attracted a lot of attention because of its ability to improve fuel economy, reduce NOx emissions and to increase torque performance over a wider rage than a conventional spark-ignition engine. In combination with microprocessor control, key functions of the motor management can be efficiently controlled by such mechatronic actuators. For moving distances between 5 and 8 mm, however, there are other actuator types with different advantages. In [P. Mercorelli and S. Liu and K. Lehmann] we presented an adaptive PID controller design for the valve actuator control based on flatness property and interval polynomials. The objective of this paper is to show:

- A model of the a hybrid actuator
- A PID-PD cascade regulator in order to avoid poor dynamic performance

The paper is organized with the following sections. Section 2 is devoted to the model description. In Section 3 an algorithm is shown to derive the control laws. The paper ends with Section 4 in which simulation results of the proposed valve using real data are presented. After that the conclusions.

2. MODELING OF THE PIEZO HYDRAULIC ACTUATOR

The proposed nonlinearity model for PEA is quite similar to these presented in [A. Adriaens et al. 2000] and in [Y.-C. Yu and M.-K. Lee 2005]. It is basically constructed from a sandwich model as shown in Fig. 1, which is based on the following hypothesis. According to the proposed

sandwich model, a PEA is constituted like a three layer sandwich. The middle layer is the effective piezo layer (P-layer), and the two outside layers connected to the electrodes are known in the literature as interfacing layers (I-layers). The P-layer is the layer that has the ordinary characteristics of piezo effects but without the nonlinearities of hysteresis and creep so that its behavior can be modeled by an equivalent linear circuitry. In contrast, the I-layers do not contribute any piezo effect; they are just part of the circuit connecting P-layer to the electrodes in series. In [Y.-C. Yu and M.-K. Lee 2005] it is

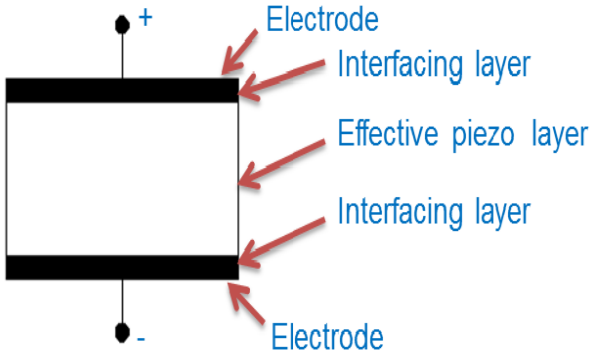

Fig. 1. The sandwich model of the PEA

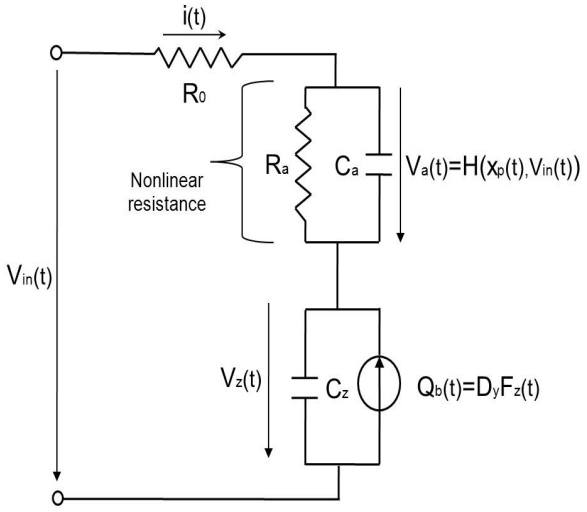

Fig. 2. Electrical part of the model

hypothesized that each of the I-layers can be equivalently represented by a capacitor and a resistor connected together in parallel. Together with the equivalent circuitry for P-layer, Fig. 2 shows the equivalent circuitry for a PEA with the I-layer nonlinearities of hysteresis and creep, in which two I-layers are combined together as C_a and R_a. The I-layer capacitor, C_a, is an ordinary capacitor, "which might be varied slightly with some factors, but here it would be assumed constant first for simplicity. The I-layer resistor, R_a , however, is really an extraordinary one with significant nonlinearity. The resistance is either fairly large, say $R_a > 10^6\ \Omega$, when the voltage $\|V_a\| < V_h$, or is fairly small, say $R_a < 1000$, when $\|V_a\| > V_h$. In [Y.-C. Yu and M.-K. Lee 2005], the threshold voltage, V_h, is defined as the hysteresis voltage of a PEA. The authors in [Y.-C. Yu and M.-K. Lee 2005] given this definition due to the observation that there is a significant difference and an abrupt change in resistance across this threshold voltage and it is this resistance difference and change across V_h that introduces the nonlinearities of hysteresis and creep in a PEA. The hysteresis effect could be seen as a function of input $V_{in}(t)$ and output $y(t)$ as follows: $H(y(t), V_{in}(t))$, see Fig. 3. According to this model, if $V_h = 0$, then the hysteresis will disappear, and if $R_a = \infty$ when $\|V_a\| < V_h$, then the creep will also disappear. Based on this proposed sandwich model and the equivalent circuitry as shown in Fig. 2, we can further derive the state model as follows:

$$\dot{V}_a(t) = -\Big(\frac{1}{R_a} + \frac{1}{R_o}\Big)\frac{V_a(t)}{C_a} - \frac{V_z(t)}{C_a R_o} + \frac{V_{in}(t)}{C_a R_o} \quad (1)$$

$$\dot{V}_z(t) = \frac{\dot{Q}_b}{C_z} + \frac{1}{C_z}\Big(-\frac{V_a(t)}{R_o} - \frac{V_z(t)}{R_o} + \frac{V_{in}(t)}{R_o}\Big), \quad (2)$$

where $Q_b = D_y F_z(t)$ is the "back electric charge force" (back-ecf) in a PEA, see [Y.-C. Yu and M.-K. Lee 2005]. According to [Y.-C. Yu and M.-K. Lee 2005] and the notation of Fig. 4, it is possible to write

$$F_z(t) = M_p/3\ddot{x}(t) + D\dot{x}(t) + Kx(t) + K_x x(t). \quad (3)$$

K and D are the elasticity and the friction constant of the spring which is antagonist to the piezo effect and it is incorporated in the PEA. C_z is the total capacitance of the PEA and R_o is the contact resistance. For further details on this model see [Y.-C. Yu and M.-K. Lee 2005]. Considering the whole system described in Fig. 4 with the assumptions of incompressibility of the oil, the whole mechanical system can be represented by a spring mass structure as shown in the conceptual schema of Fig. 4. In this system the following notation is adopted: K_x is the elasticity constant factors of the PEA. In the technical literature, factor $D_x K_x = T_{em}$ is known with the name "transformer ratio" and states the most important characteristic of the electromechanical transducer. $M_p/3$ is, in our case, the moving mass of the piezo structure which is a fraction of whole piezo mass, M_{SK} is the sum of the mass of the piston with the oil and the moving actuator and M_v is the mass of the valve. It is possible to notice that the moving mass of the piezo structure is just a fraction of the whole piezo mass. The value of this fraction is given by the constructer of the piezo device and it is determined by experimental measurements. K_{SK} and D_{SK} are the characteristics of the antagonist spring to the mechanical servo valve, see Fig. 4. D_{oil} is the friction constant of the oil. Moreover, according to [Y.-C. Yu and M.-K. Lee 2005], motion $x_p(t)$ of diagram in Fig. 3 is

$$x_p(t) = D_x V_z(t). \quad (4)$$

According to diagram of Fig. 2, it is possible to write as follows:

$$V_z = V_{in}(t) - R_0 i(t) - H(x_p(t), V_{in}(t)), \quad (5)$$

where R_0 is the connection resistance and $i(t)$ is the input current as shown in Fig. 2. $H(x_p(t), V_{in}(t))$ is the function which describes the hysteresis effect mentioned above and shown in the simulation of Fig. 3. Considering the whole system described in Fig. 4, the electrical and mechanical systems described in Figs. 2, 3 and 4 can be represented by the following mathematical expressions:

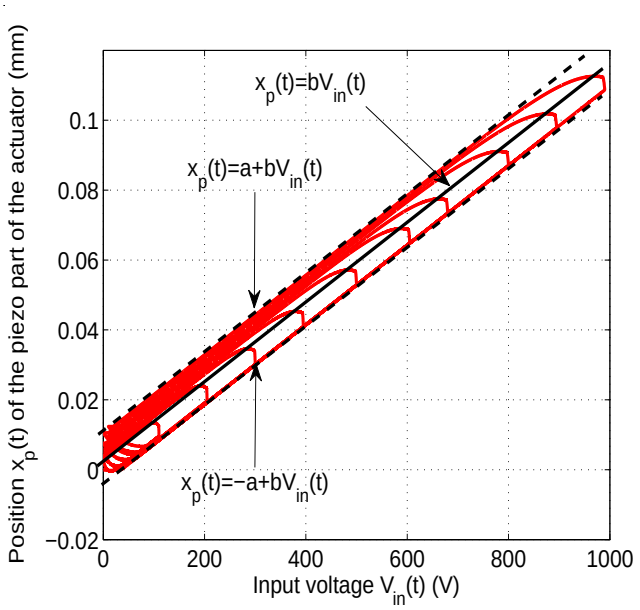

Fig. 3. Simulated Hysteresis curve of the piezo part of the actuator: $H(x_p(t), V_{in}(t))$

$$\frac{M_p}{3}\ddot{x}(t) + M_{SK}\ddot{x}_{SK}(t) + Kx(t) + D\dot{x}(t) + K_{SK}x_{SK}(t) + D_{SK}\dot{x}_{SK}(t) + D_{oil}\dot{x}_{SK}(t) + K_x\Big(x(t) - \Delta x_p(V_{in}(t))\Big) = 0, \quad (6)$$

where $\Delta x_p(t)$ represents the interval function of $x_p(t)$ as shown in Fig. 3 which, according to equation (4), can be expressed as

$$\Delta x_p(t) = D_x \Delta V_z(t), \quad (7)$$

Finally, using equations (5) and (7),

$$K_x \Delta x_p(t) = K_x D_x\big(V_{in}(t) - R_0 i(t) - H(\Delta x_p(t), V_{in}(t))\big), \quad (8)$$

which represents the interval force generated by the piezo device. Equation (6) can be expressed in the following way:

$$\frac{M_p}{3}\ddot{x}(t) + M_{SK}\ddot{x}_{SK}(t) + Kx(t) + D\dot{x}(t) + K_{SK}x_{SK}(t) + D_{SK}\dot{x}_{SK}(t) + D_{oil}\dot{x}_{SK}(t) + K_x x(t) = K_x \Delta x_p(V_{in}(t)). \quad (9)$$

It is to be noticed that the following relationship holds:

$$x_{SK}(t) = Wx(t), \quad (10)$$

where W is the position ratio above defined and it states the incompressibility of the oil in the conic chamber. The following equation completes the dynamic of the considered system:

$$M_v\ddot{y}(t) + D_{oil}\dot{y}(t) = F\big(x_{SK}(t), y(t)\big) - F_d(t). \quad (11)$$

According to Fig. 4, $x(t)$ is the position of the piezo actuator, $x_{SK}(t)$ is the position of the mechanical servo actuator, $y(t)$ represents the position of the valve. Function $F(x_{SK}(t), y(t))$ represents the force exerted by the pump on surface S of the armature of the moving valve, see Fig 4. Moreover,

$$F(x_{SK}(t), y(t)) = (p_A(t) - p_B(t))S, \quad (12)$$

where $p_A(t)$ and $p_B(t)$ are the pressure in the two oil chambers separated by the armature of the valve. In [H. Murrenhoff] pressure $p_A(t)$ and $p_B(t)$ are nonlinear functions of the mechanical servo valve position $y(t)$. The linearization of this function at each desired position $y_d(t)$ will be considered later. $F_d(t)$ is the combustion back pressure in terms of force. According to Fig. 3 in which

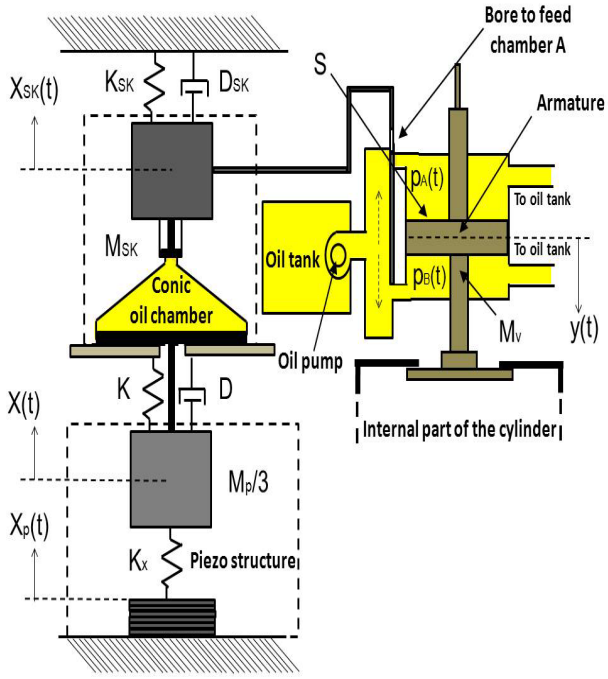

Fig. 4. Mass spring model of the whole actuator

an upper bound and a lover bound of the hysteresis curve is indicated, it is possible to write that

$$\Delta x_p(V_{in}(t)) = [-a \quad a] + bV_{in}(t), \quad (13)$$

with $a \in \mathbb{R}$ and $b \in \mathbb{R}$ two positive constants are indicated. In particular,

$$\underline{\Delta} x_p(V_{in}(t)) = -a + bV_{in}(t), \quad (14)$$

and

$$\overline{\Delta} x_p(V_{in}(t)) = a + bV_{in}(t). \quad (15)$$

Considering this notation, the system represented in (6) can be split into the following two systems:

a)

$$\frac{M_p}{3}\ddot{x}(t) + M_{SK}\ddot{x}_{SK}(t) + Kx(t) + D\dot{x}(t) + K_{SK}x_{SK}(t) + D_{SK}\dot{x}_{SK}(t) + D_{oil}\dot{x}_{SK}(t) + K_x x(t) = \underline{\Delta} x_p(V_{in}(t)), \quad (16)$$

b)

$$\frac{M_p}{3}\ddot{x}(t) + M_{SK}\ddot{x}_{SK}(t) + Kx(t) + D\dot{x}(t) + K_{SK}x_{SK}(t) + D_{SK}\dot{x}_{SK}(t) + D_{oil}\dot{x}_{SK}(t) + K_x x(t) = \overline{\Delta} x_p(V_{in}(t)), \quad (17)$$

3. A PID-PD CONTROLLER AS TWO SLIDING MODE SURFACES

Figure 3 shows the proposed control structure. It is possible to see how a feedforward structure is present in order to achieve a regulation around the desired trajectory. An internal PD structure and an externan PID structure complete the whole control scheme to guarantee the robustness.

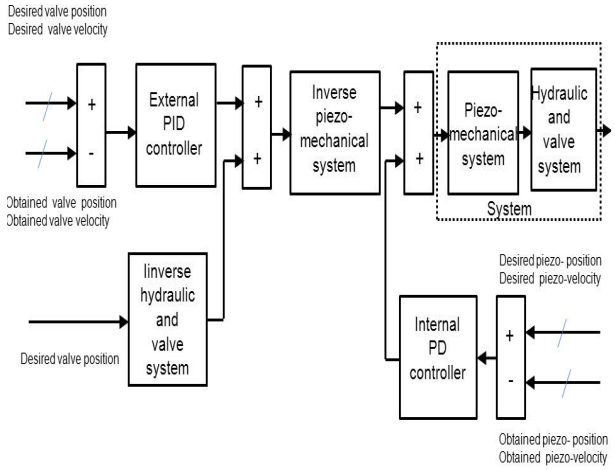

Fig. 5. Proposed cascade PID-PD structure

3.1 Internal PD controller

The PD control structure presented in this section is quite similar to the sliding control structure presented in [J. Lee et al. 2010]. Considering Figs. 2 and 4, if the dynamics shown in (16) and (17) is considered in a state space representation, then

$$\dot{x}_1(t) = x_2(t) \tag{18}$$

$$\dot{x}_2(t) = \frac{-Dx_2(t) - (K + K_x + K_{SK}W)x_1(t) + 3K_x b V_{in}(t)}{\frac{M_p}{3} + M_{SK}W} + \frac{(-1)^q a}{\frac{M_p}{3} + M_{SK}W} \tag{19}$$

where $q = 1, 2..$ The system represented in equations (18) and (19) can be represented as follows:

$$\begin{bmatrix} \dot{x}_1(t) \\ \dot{x}_2(t) \end{bmatrix} = \mathbf{f}(\mathbf{x}(t), H\big(y(t), V_{in}(t)\big)) + \mathbf{B}V_{in}(t), \tag{20}$$

where it is assumed that $V_{in}(t) = V_z(t)$,

$$\mathbf{f}(\mathbf{x}(t), H\big(y(t), V_{in}(t)\big)) = \begin{bmatrix} x_2(t) \\ \dfrac{-Dx_2(t) - (K + K_x + K_{SK}W)x_1(t)}{\frac{M_p}{3} + M_{SK}W} \end{bmatrix}, \tag{21}$$

and $\mathbf{B} = \begin{bmatrix} 0 \\ \dfrac{3K_x b + (-1)^q a}{\frac{M_p}{3} + M_{SK}W} \end{bmatrix}$. The following PD controller is defined:

$$K(t) = \mathbf{G}\big(\mathbf{x}_d(t) - \mathbf{x}(t)\big), \tag{22}$$

where $\mathbf{G} = [\, P_i \;\; D_i \,]$, and $\mathbf{x}_d(t)$ represents the vector of the desired piezo trajectories. Equation (22) becomes as follows:

$$K_i(t) = [\, P_i \;\; D_i \,] \begin{bmatrix} x_{1d}(t) - x_1(t) \\ x_{2d}(t) - x_2(t) \end{bmatrix}, \tag{23}$$

thus

$$K_i(t) = P_i\big(x_{1d}(t) - x_1(t)\big) + D_i\big(x_{2d}(t) - x_2(t)\big), \tag{24}$$

P_i and D_i are the internal P and the intern D parameters of the PD controller. If the following Lyapunov function is defined:

$$V(K_i) = \frac{K_i^2(t)}{2}, \tag{25}$$

then it follows that:

$$\dot{V}(K_i) = K_i(t)\dot{K}_i(t). \tag{26}$$

In order to find the stability of the solution $s(t) = 0$, it is possible to choose the following function:

$$\dot{V}(K_i) = -\eta(t){K_i}^2(t), \tag{27}$$

with $\eta > 0$. Comparing (26) with (27), the following relationship is obtained:

$$K_i(t)\dot{K}_i(t) = -\eta K_i^2(t), \tag{28}$$

and finally

$$K_i(t)\big(\dot{K}_i(t) + \eta K_i(t)\big) = 0. \tag{29}$$

The no trivial solution follows from the condition

$$\dot{K}_i(t) + \eta K_i(t) = 0. \tag{30}$$

From (22) it follows:

$$\dot{K}_i(t) = \mathbf{G}\big(\dot{\mathbf{x}}_d(t) - \dot{\mathbf{x}}(t)\big) = \mathbf{G}\dot{\mathbf{x}}_d(t) - \mathbf{G}\dot{\mathbf{x}}(t). \tag{31}$$

The main idea is to find a $u_{eq}(t)$, an equivalent input, and after that a $V_{in}(t)$, such that $\dot{\mathbf{x}}(t) = \dot{\mathbf{x}}_d(t)$. For that, from (20) it follows that:

$$\dot{\mathbf{x}}(t) = \dot{\mathbf{x}}_d(t) = \mathbf{f}(x_d(t), H) + \mathbf{B}V_{in}(t), \tag{32}$$

and from (31) the following relationship is obtained:

$$\dot{K}_i(t) = \mathbf{G}\dot{\mathbf{x}}_d(t) - \mathbf{G}\mathbf{f}(x_d(t), H) - \mathbf{G}\mathbf{B}V_{in}(t) = \mathbf{G}\mathbf{B}\big(u_{eq}(t) - V_{in}(t)\big), \tag{33}$$

where $u_{eq}(t)$ is the equivalent input which, in our case, assumes the following expression:

$$u_{eq}(t) = \big(\mathbf{G}\mathbf{B}\big)^{-1}\mathbf{G}\Big(\dot{\mathbf{x}}_d(t) - \mathbf{f}(x_d(t), H)\Big). \tag{34}$$

After inserting (33) in (30) the following relationship is obtained:

$$\mathbf{G}\mathbf{B}\big(u_{eq}(t) - V_{in}(t)\big) + \eta K_i(t) = 0, \tag{35}$$

and in particular

$$V_{in}(t) = u_{eq}(t) + \big(\mathbf{G}\mathbf{B}\big)^{-1}\eta K_i(t). \tag{36}$$

Normally it is a difficult job to calculate $u_{eq}(t)$. If equation (33) is rewritten in a discrete form using explicit Euler approximation, then it follows:

$$\frac{K_i((k+1)T_s) - K_i(kT_s)}{T_s} = \mathbf{G}\mathbf{B}\big(u_{eq}(kT_s) - V_{in}(kT_s)\big). \tag{37}$$

If equation (36) is also rewritten in a discrete form, then

$$V_{in}(kT_s) = u_{eq}(kT_s) + \big(\mathbf{G}\mathbf{B}\big)^{-1}\eta K_i(kT_s). \tag{38}$$

Equation (37) can be also rewritten as

$$u_{eq}(kT_s) = V_{in}(kT_s) + \big(\mathbf{G}\mathbf{B}\big)^{-1}\frac{K_i((k+1)T_s) - K_i(kT_s)}{T_s}. \tag{39}$$

Equation (39) can be estimated to one-step backward in the following way:

$$u_{eq}((k-1)T_s) = V_{in}((k-1)T_s) + \big(\mathbf{G}\mathbf{B}\big)^{-1}\frac{K_i(kT_s) - K_i((k-1)T_s)}{T_s}. \tag{40}$$

Because of function $u_{eq}(t)$ is a continuous one, we can write

$$u_{eq}(kT_s) \approx u_{eq}((k-1)T_s). \tag{41}$$

Considering equation (41), then equation (40) becomes

$$u_{eq}(kT_s) = V_{in}((k-1)T_s) + \left(\mathbf{GB}\right)^{-1} \frac{K_i(kT_s) - K_i((k-1)T_s)}{T_s}. \quad (42)$$

Inserting (42) into (38)

$$V_{in}(kT_s) = V_{in}((k-1)T_s) + \left(\mathbf{GB}\right)^{-1} \left(\eta K_i(kT_s) + \frac{K_i(kT_s) - K_i((k-1)T_s)}{T_s}\right), \quad (43)$$

and finally

$$V_{in}(kT_s) = V_{in}((k-1)T_s) + \left(\mathbf{GB}T_s\right)^{-1} \left(\eta T_s K_i(kT_s) + K_i(kT_s) - K_i((k-1)T_s)\right). \quad (44)$$

3.2 External PID controller

If the following external PID is defined

$$s_e(t) = [\, P_e \;\; D_e \;\; I_e \,] \begin{bmatrix} x_{1vd}(t) - x_{1v}(t) \\ x_{2vd}(t) - x_{2v}(t) \\ \int (x_{1d}(t) - x_1(t))dt \end{bmatrix}, \quad (45)$$

where $\mathbf{x}_{vd}(t)$ represents the vector of the desired valve trajectories. Then after similar calculation the following PID structure is calculated:

$$V_{in}(kT_s) = V_{in}((k-1)T_s) + \left(\mathbf{HL}T_s\right)^{-1} \left(\eta T_s K_i(kT_s) + K_e(kT_s) - K_e((k-1)T_s)\right). \quad (46)$$

The following notation is used: $\mathbf{G} = [\, P_e \;\; D_e \;\; I_e \,]$ and

$$\mathbf{H} = \begin{bmatrix} 0 \\ -F(x_{SK_d}(t)y_d(k))/M_v \end{bmatrix}. \quad (47)$$

where $c_{x_{SK_d}(k)} \in \mathbb{R}$ and $c_{y_d(k)} \in \mathbb{R}$ are the constants which come from the linearization of $F(x_{SK}(t), y(t))$ at each t-time.

4. SIMULATIONS RESULTS

The control law of equation (44) is tested using the model described in section 2. Figure 6 shows the final result concerning the tracking of a desired position of an exhaust valve with 8000 rpm. Figure 7 shows the final result concerning the tracking of a desired velocity of an exhaust valve with 8000 rpm. Figure 8 shows the profile of the simulated force on the piezo part of the proposed actuator. But, the force acting directly on the valve at the opening time has a pick value equal to 700 N circa and it is reduced to a few newtons acting on the piezo part thanks to the decoupling structure of the hybrid actuator. This is one of the greatest advantages of these hybrid actuators. The model of a such kind of disturbance is obtained as an exponent function of the position of the valve. The digital controller is set to work with a sampling time equal to 20×10^{-6} s, according to the specifications of the Digital Signal Processor which we are intended to test the system with.

Remark 1. It is to remark that, equation (44) states that the control law does not depend on the dynamics of the system model. The control law depends for the internal PD controller just on the moving mass and on product $K_x D_x$

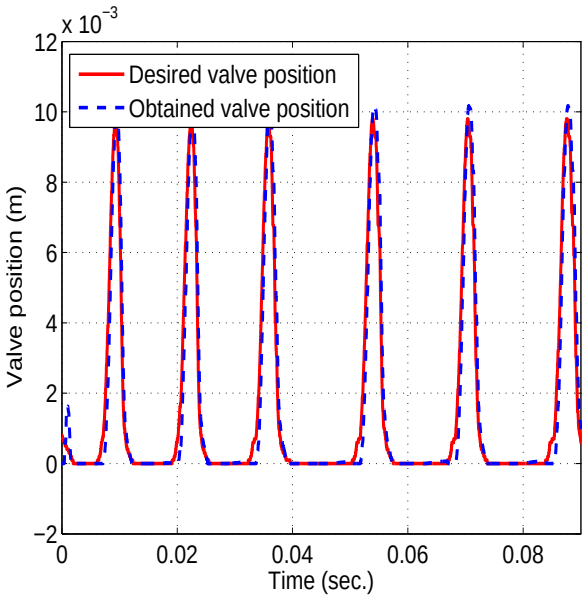

Fig. 6. Desired and obtained valve positions corresponding to 8000 rpm

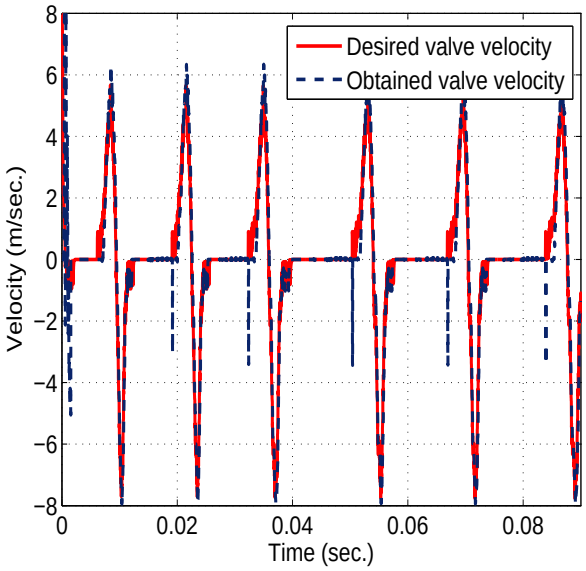

Fig. 7. Desired and obtained valve velocity (8000 rpm)

(transformer ratio). All these parameters are always well known in a piezoelectric actuator. Product $K_x D_x$ depends on the temperature, the piezoelectric actuator is equipped with a temperature sensor which activates an air cooling system. Concerning to external PID controller the control law depends on the moving mass and on the pressures of the two oil chambers, and on the valve surface.

5. CONCLUSIONS AND FUTURE OBJECTIVES

5.1 Conclusions

This paper deals with a hybrid actuator composed by a piezo and a hydraulic part and its control structure for camless engine motor applications. The idea is to use the

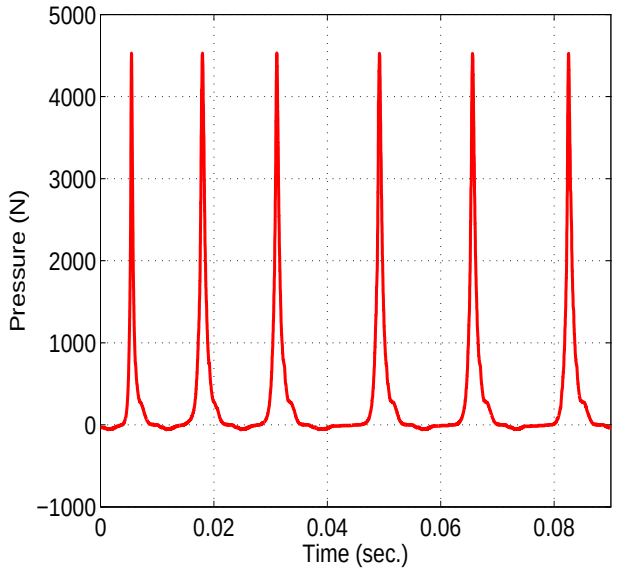

Fig. 8. Force of the internal combustion considering 8000 rpm

advantages of both, the high precision of the piezo and the force of the hydraulic part. In the control problem nonlinearities such as hysteresis, saturations, and creep are taken into account. Simulations with real data of motor and of a piezo actuator are shown.

5.2 Future Works

Future works include an adaptive PID-PD control structure and measurements on an experimental setup. Some refined models of the whole structure are already under consideration. In particular, in the presented paper it is assumed that the oil of the hydraulic part is incompressible. This assumption should be removed and the pressure of the oil should be considered as a further state variable which the system can be described with.

REFERENCES

[W. Hoffmann and A. G. Stefanopoulou 2001] terative learning control of electromechanical camless valve actuator. In Proc. of American control conference, 2001.

[P. Mercorelli 2009] endering the elecreomechanical valve actuator globally asymptotically stable. In Proc. 42nd IEEE Conference on Decision and Control, Maui, 2003.

[C.-T. Li and Y.-H. Tan 2005] n antisaturating adaptive preaction and a slide surface to achieve soft landing control for electromagnetic actuators. To appear on IEEE/ASME Transactions on Mechatronics, Already available in early access article of the IEEE, ISSN :1083-4435, 2011.

[D. Croft et al. 2001] reep, hysteresis, and vibration compensation for piezoactuators: Atomic force microscopy application. Transactions of the ASME Journal of Dynamic Systems, Measurement, and Control, 123(1):3543, 2001.

[B. Jayawardhana et al. 2007] ID control of secondorder systems with hysteresis. In Proceedings of the 46th IEEE Conference on Decision and Control, pages 46264630, 2007.

[C.-T. Li and Y.-H. Tan 2005] daptive output feedback control of systems preceded by the preisach-type hysteresis. IEEE Transactions on Systems Man, and Cybernetics, Part B: Cybernetics, 35(1):130135, 2005.

[G. Bertotti 1992] ynamic generalization of the scalar preisach model of hysteresis. IEEE Transaction on Magnetics, 28(5 pt 2):25992601, 1992.

[R. Bouc 1967] orced vibration of mechanical systems with hysteresis. In Proceedings of the Conference on Nonlinear Oscillation, 1967.

[J. Lee et al. 2010] Precise tracking control of piezo actuator using sliding mode control with feedforward compensation. In Proceedings of the SICE Annual Conference 2010, 2010.

[P. Mercorelli 2009] obust feedback linearization using an adaptive PD regulator for a sensorless control of a throttle valve. Mechatronics a journal of IFAC. Elsevier publishing, 19(8):13341345, 2009.

[A. Adriaens et al. 2000] Modeling piezoelectric actuators. IEEE/ASME Transactions on Mechatronics, 5(4):331341, 2000.

[Y.-C. Yu and M.-K. Lee 2005] A dynamic nonlinearity model for a piezo-actuated positioning system. In Proceedings of the 2005 IEEE International Conference on Mechatronics, 2005.

[P. Mercorelli and S. Liu and K. Lehmann] Robust Flatness Based Control of an Electromagnetic Linear Actuator Using Adaptive PID Controller. In Proceedings of the 42nd IEEE Conference on Decision and Control (Hawaii, (USA)). Hyatt Regency Maui, Hawaii, (USA),2003.

[H. Murrenhoff] Servohydraulik. Shaker Verlag publishing. Aachen (Germany), 2002.